Use of Nanoindentation, Finite Element Simulations, and a Combined Experimental/Numerical Approach to Characterize Elastic Moduli of Individual Porous Silica Particles

ARTICLE *in* PARTICULATE SCIENCE AND TECHNOLOGY · OCTOBER 2014

Impact Factor: 0.52 · DOI: 10.1080/02726351.2014.950396

6 AUTHORS, INCLUDING:

Sushir Simkhada

Hysitron, Incorporated

1 PUBLICATION **0** CITATIONS

SEE PROFILE

Qin Yu

Oregon State University

33 PUBLICATIONS **405** CITATIONS

SEE PROFILE

Hyung-Ick Kim

University of Delaware

36 PUBLICATIONS **72** CITATIONS

SEE PROFILE

Particulate Science and Technology: An International Journal
Publication details, including instructions for authors and subscription information:
http://www.tandfonline.com/loi/upst20

Use of Nanoindentation, Finite Element Simulations, and a Combined Experimental/Numerical Approach to Characterize Elastic Moduli of Individual Porous Silica Particles

Ronald F. Gibson[a], Hong-Kyu Jang[b], Sushir Simkhada[c], Qin Yu[a], Hyung-Ick Kim[d] & Jonghwan Suhr[e]

[a] Department of Mechanical Engineering, University of Nevada, Reno, NV, USA

[b] Composites Research Center, Korea Institute of Materials Science, Changwon, South Korea

[c] Hysitron, Inc., Minneapolis, MN, USA

[d] Manufacturing Process Technology Innovation Center, Korea Institute of Industrial Technology, Gyeongsangnam-do, South Korea

[e] Department of Polymer Science & Engineering and Department of Energy Science, Sungkyunkwan University, Suwon, South Korea

Accepted author version posted online: 02 Sep 2014.Published online: 02 Sep 2015.

To cite this article: Ronald F. Gibson, Hong-Kyu Jang, Sushir Simkhada, Qin Yu, Hyung-Ick Kim & Jonghwan Suhr (2015) Use of Nanoindentation, Finite Element Simulations, and a Combined Experimental/Numerical Approach to Characterize Elastic Moduli of Individual Porous Silica Particles, Particulate Science and Technology: An International Journal, 33:2, 213-218, DOI: 10.1080/02726351.2014.950396

To link to this article: http://dx.doi.org/10.1080/02726351.2014.950396

Particulate Science and Technology, 33: 213–218

ISSN: 0272-6351 print/1548-0046 online
DOI: 10.1080/02726351.2014.950396

Taylor & Francis
Taylor & Francis Group

Use of Nanoindentation, Finite Element Simulations, and a Combined Experimental/Numerical Approach to Characterize Elastic Moduli of Individual Porous Silica Particles

RONALD F. GIBSON,[1] HONG-KYU JANG,[2] SUSHIR SIMKHADA,[3] QIN YU,[1] HYUNG-ICK KIM,[4] and JONGHWAN SUHR[5]

[1]*Department of Mechanical Engineering, University of Nevada, Reno, NV, USA*
[2]*Composites Research Center, Korea Institute of Materials Science, Changwon, South Korea*
[3]*Hysitron, Inc., Minneapolis, MN, USA*
[4]*Manufacturing Process Technology Innovation Center, Korea Institute of Industrial Technology, Gyeongsangnam-do, South Korea*
[5]*Department of Polymer Science & Engineering and Department of Energy Science, Sungkyunkwan University, Suwon, South Korea*

This article describes the use of a combination of experimental nanoindentation and finite element numerical simulations to indirectly determine the elastic modulus of individual porous, micron-sized silica (SiO_2) particles. Two independent nanoindentation experiments on individual silica particles were employed, one with a Berkovich pyramidal nanoindenter tip, the other with a flat punch nanoindenter tip. In both cases, 3D finite element simulations were used to generate nanoindenter load–displacement curves for comparison with the corresponding experimental data, using the elastic modulus of the particle as a curve-fitting parameter. The resulting indirectly determined modulus values from the two independent experiments were found to be in good agreement, and were considerably lower than the published values for bulk or particulate solid silica. The results are also consistent with previously reported modulus values for nanoindentation of porous thin film SiO_2. Based on a review of the literature, the authors believe that this is the first article to report on the use of nanoindentation and numerical simulations in a combined experimental/numerical approach to determine the elastic modulus of individual porous silica particles.

Keywords: Elastic, finite element, moduli, nanoindentation, porous silica

1. Introduction

Silica (silicon dioxide, or SiO_2) particles have been used for many years as nonstructural fillers for plastics, where their low thermal expansion coefficient, low thermal conductivity, low density, low cost, and compatibility with a variety of polymer resins make them very attractive (Wypych 2010). Depending on their shape, silica particles may also be useful for structural reinforcement in polymer composites. More recently, silica nanoparticles are being used to enhance the structural properties of conventional fiber-reinforced composites in a new class of composites known as hybrid multiscale composites (Uddin and Sun 2008; Manjunatha et al. 2009). Characterization of physical properties of silica particles has been the subject of several investigations, including indirect determination of elastic moduli by combined experimental/numerical approaches. Such procedures involve either tensile test experiments (Jang et al. 2013) or nanoindentation (Yan et al. 2011) of both silica-reinforced polymers and the corresponding neat polymer resins, along with finite element numerical simulations of the experiments using the particle modulus as a curve-fitting parameter. Direct nanoindentation of large diameter (155–476 μm) crystalline pharmaceutical powders using the method of Oliver and Pharr (1992) has been reported by Taylor et al. (2004), but nanoindentation of small (~10 μm) diameter individual porous silica particles combined with numerical simulation for indirect determination of the particle Young's modulus has not been explored.

Due to its low dielectric constant, low density, low thermal conductivity, and high surface area, porous silica in the form of particles, films, or coatings has many potential applications, such as microelectronic interconnects (Jain et al. 2001), thermal insulators (Coquard et al. 2013), antireflective coatings (Karasinski et al. 2011), and acoustic attenuators (Caponi et al. 2003). While the presence of pores

Address correspondence to: Ronald F. Gibson, Department of Mechanical Engineering, University of Nevada, Reno, NV 89557-0312, USA. E-mail: ronaldgibson@unr.edu

Color versions of one or more of the figures in the article can be found online at www.tandfonline.com/upst.

in these materials leads to desirable properties such as low dielectric constant, low density, low thermal conductivity, and high surface area, the same pores cause reductions in elastic properties such as Young's modulus, and the study of such behavior calls for experimental work. In addition, development of analytical models for predicting elastic behavior of these materials depends in part on the availability of experimental data for comparison with predictions. Thus, experimental characterization of elastic properties such as Young's modulus of porous silica particles is of considerable interest, and is the focus of the research reported here. Others have previously reported on the use of nanoindentation to characterize elastic properties of porous silica films (Huang and Pelegri 2003; Chang and Huang 2006; Herrmann et al. 2006; Herrmann et al. 2008), and scanning force microscopy has been employed to determine elastic properties of porous nanosilica coatings (Vincent et al. 2007), but to the best of the authors' knowledge, the use of nanoindentation, numerical simulations, and a combined experimental/numerical approach to characterize the Young's modulus of individual porous silica particles has not been previously reported in the literature.

2. Experiments and Simulations

Spherical particles of porous silica having an average diameter of 10 μm and an average pore size of 2 nm (Figure 1) were obtained from ABC Nanotech in South Korea. Nanoindentation of individual particles (Figure 2) was conducted using Hysitron TI 950 TriboIndenter Nanomechanical Test Instruments (Hysitron web site 2014) located at the University of Nevada, Reno in Reno, Nevada and at Hysitron, Inc. in Minneapolis, Minnesota. The nanoindentation experiments at the University of Nevada, Reno were conducted with a Berkovich pyramidal indenter tip [Figures 2 and 3(a)] (University of Nebraska web site 2014), while the tests at Hysitron were conducted with a flat-ended conical punch tip [Figures 2 and 3(b)] (Simha et al. 2007). In both cases, experimental load–penetration depth curves were generated for comparison with the corresponding results from finite element simulations, using the Young's modulus of the particle as a curve-fitting parameter in the simulations. Experimental penetration rate or

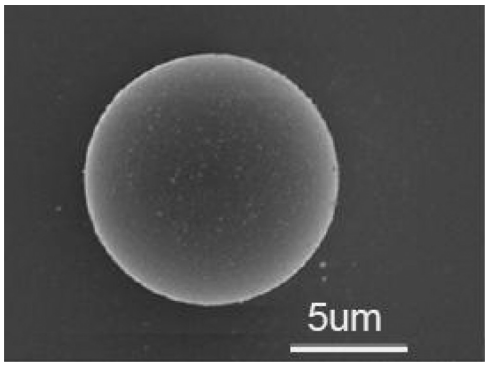

Fig. 1. SEM image of 10 μm nominal diameter porous SiO_2 particle with randomly distributed pores of nominal size 2 nm.

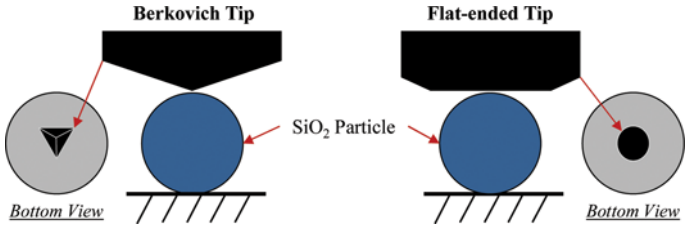

Fig. 2. Illustration of experimental setup for nanoindentation of SiO_2 particles.

indentation rate is approximately 200 nm/s, which roughly corresponds to a strain rate of 0.02/s over a 10-μm diameter particle. This seems to be a reasonable strain rate for a ceramic material, since nanoindentation of various ceramics has been conducted at strain rates of 0.04/s by Page et al. (1992); 0.01/s to 0.1/s by Bhakri et al. (2012); and 0.025/s to 0.125/s by Vandeperre et al. (2010). Comparisons of experimental and predicted load–depth curves were done for the case of penetration depth control.

Finite element simulations were conducted by one of the co-authors, Dr. Jang, when he was located at the University of Delaware using the ABAQUS 6.11 commercial finite element software under the assumption of elastic behavior. Figure 4 shows the finite element model for the Berkovich indenter and particle, while Figure 5 shows the corresponding simulation for the flat-ended conical punch indenter and particle. The models in Figures 4 and 5 were developed using CAX4R 4-node bilinear axisymmetric quadrilateral elements. For purposes of illustration and visualization, the mesh sizes shown in Figures 4 and 5 are larger than the actual mesh sizes. In the actual FEA models of Figures 4 and 5, the number of elements for both SiO_2 particles is

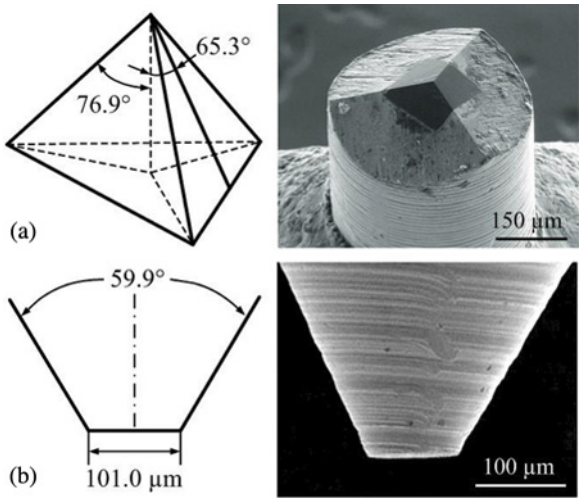

Fig. 3. (a) Berkovich pyramidal (permission granted by University of Nebraska to reproduce image from web site http://bm3.unl.edu/hysitron-nanoindenter#details and (b) flat-ended conical (permission granted by American Society of Mechanical Engineers to reproduce image from Simha, et al (2007)) nanoindenter probes.

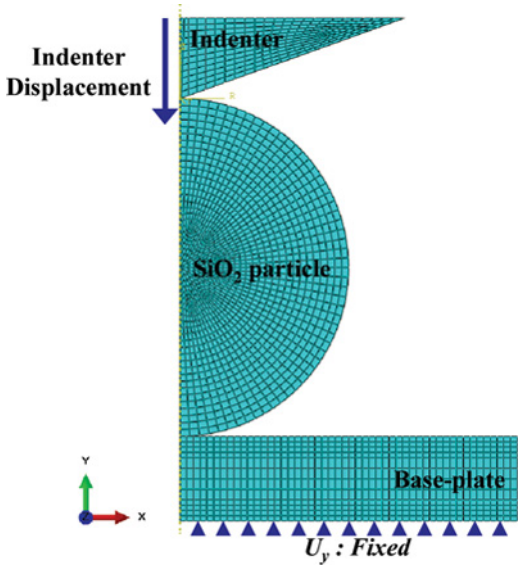

Fig. 4. Axisymmetric finite element model for Berkovich indenter and SiO_2 particle.

4,284 and the Berkovich indenter with a tip radius of 100 nm has 3,693 elements (flat-ended indenter: 1,798 elements). In addition, the contact surface between the SiO_2 particle and the indenter involves a fine mesh, and the element size of the Berkovich tip is much smaller than that of the SiO_2 particle. Surface-to-surface contact at the indenter/particle and particle/base plate interfaces was modeled with the "Hard Contact" condition in ABAQUS, which minimized the penetration of the slave surface into the master surface at the constraint locations, and it did not allow the transfer of tensile stress across the interface. The assumed Young's modulus and Poisson's ratio for the diamond indenter, the silica particle, and the steel base plate are listed in Table 1, where the assumed Young's modulus for the silica particle was varied to find the best agreement between experimental and simulated nanoindenter load–depth curves. Due to the lack of data on Poisson's ratio for porous silica, the Poisson's ratio for solid silica was used. Since the horizontal (or transverse) displacements of the particle are not constrained during the indentation test, the value of the particle Poisson's ratio is not expected to have a significant effect on the indenter load–displacement relationship along the vertical direction. The indenter and particle displacements were assumed to be free to move along the Y-direction (the axis of symmetry), while the baseplate and bottom surface of the particle were assumed to be fixed against displacements along the Y-direction. Due to the use of axisymmetric elements, the pyramidal shape of the Berkovich indenter tip had to be approximated as an axisymmetric equivalent cone (Figure 4) having a semiapical angle (half angle) of 70.3° (Bucaille and Felder 2002). The semiapical angle of 70.3° is selected so that the volume of the equivalent cone is equal to that of the Berkovich indenter for a given penetration depth (Bucaille and Felder 2002). Due to the random shapes and sizes of the pores, porosity of the particles could not be included in the simulations, and particles were assumed to be solid spheres. As a result, the particle modulus values found from the experiments and simulations can be taken as effective moduli of equivalent homogeneous particles.

Table 1. Properties used in finite element simulations

Material	Young's modulus (GPa)	Poisson's ratio
Diamond indenter tip	1,200[a]	0.2[a]
Silica particle	Varied[b]	0.17[c]
Steel base plate	180[d]	0.3[e]

[a]http://www.chm.bris.ac.uk/motm/diamond/diamprop/htm.
[b]Particle Young's modulus used as a curve-fitting parameter in the finite element simulations.
[c]http://www.accuratus.com/fused.html.
[d]http://www.engineeringtoolbox.com/young-modulus-d_417/html.
[e]http://www.engineeringtoolbox.com/metals-poissons-ratio-d_1268.html.

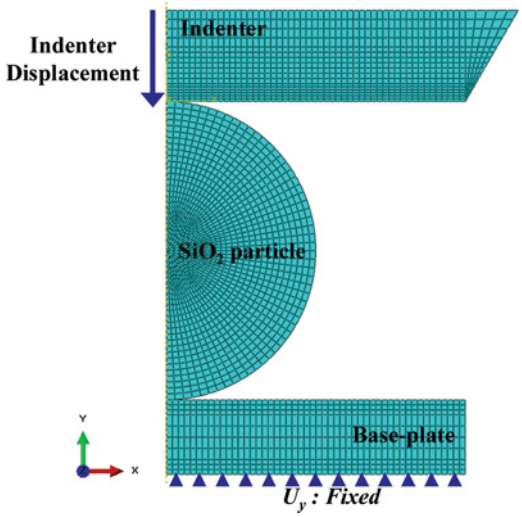

Fig. 5. Axisymmetric finite element model for flat-ended conical indenter and SiO_2 particle.

3. Results and Conclusions

Due to the difficulty in precisely aligning the Berkovich tip with the centerline of the particle, and in order to get a feel for the sensitivity of the experiments to possible misalignment, 3D half domain finite element simulations were developed for cases where the tip offset was 0°, 5°, 10°, and 15° with respect to the vertical centerline of the particle. Figure 6 shows such a model for the case of a 10° offset. For these models, it was not possible to use axisymmetric elements, so type C3D8R (8-node linear 3D brick) elements and a half domain model were used. The top surface of the indenter was fixed against displacements along the X- and Z-directions and free to move along the Y-direction, while the bottom surface of the particle was fixed against movement along X-, Y-, and Z-directions. For all of the tip offset simulations, the particle modulus was assumed to be 3 GPa, which had been found to be a reasonable value based on the experiments and simulations described in

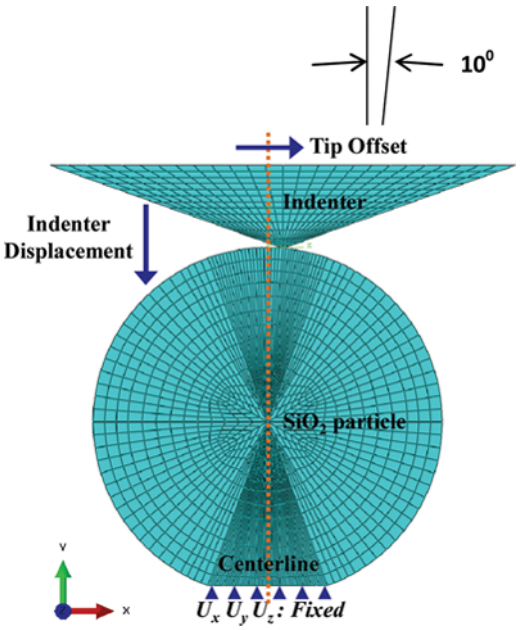

Fig. 6. 3D half domain finite element model for 10° offset Berkovich indenter and SiO_2 particle.

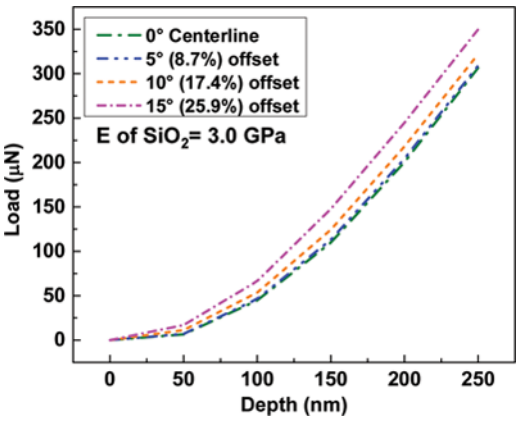

Fig. 7. Predicted load–depth curves for offset Berkovich indenter simulations (see Figure 6) with tip offsets of 0°, 5°, 10°, and 15° from vertical centerline of SiO_2 particle.

Figures 4 and 5. Predicted load–depth curves for offset Berkovich indenter simulations with tip offsets of 0°, 5°, 10°, and 15° are shown in Figure 7. It is seen that the required indenter load for a given penetration depth increases slightly with increased offset, probably because of the increased contact area between the particle and the indenter tip. In this paper, the penetration depth is defined as the distance between the initial contact point and the final deformed point on the SiO_2 particle (Figure 8). In addition, the boundary condition between the indenter tip and the SiO_2 particle was assumed to be nonslip, and the contact area was calculated by the post-processing of ABAQUS 6.11. According to the calculated values, the contact area was changed from 0.805 to 1.290 μm^2 with the increase in offset angle from 0° to 15°. As a result, the required indenter load for a given penetration depth increases slightly with the increased offset. The resulting uncertainty due to possible tip offset should be kept in mind when interpreting the curve-fitting analysis in Figure 9.

As mentioned earlier, the main objective of this research was to compare experimental load–penetration depth curves with the corresponding finite element simulations, using the unknown Young's modulus of the particle as a curve-fitting parameter in the simulations. Figures 9 and 10 show such comparisons for the Berkovich and flat-ended conical tips, respectively. Due to the extreme difficulty in aligning the Berkovich tip with the particle centerline and preventing slip and/or rolling of the particle during the test, only one satisfactory experiment was conducted with the Berkovich tip as shown in Figure 9. Particle slip and/or rolling may be responsible for the deviation in the experimental load–depth curve in Figure 9 above about 175 nm, so only the portion of the curve below 175 nm was considered in the curve-fitting analysis. A tip offset of zero was assumed in the finite element predictions shown in Figure 9, but the actual tip offset is unknown. The flat-ended conical tip presented fewer difficulties, so three experiments were conducted and the curve in Figure 10 represents an average of the three tests. For the three tests, the coefficient of variation (or standard deviation divided by the mean) for the ratio of the experimental peak force to the corresponding penetration depth was approximately 0.16. Both types of tests were conducted under penetration depth control. Based on the two independent tests, the best-fit value of the effective particle modulus for small penetration depths seems to be in the

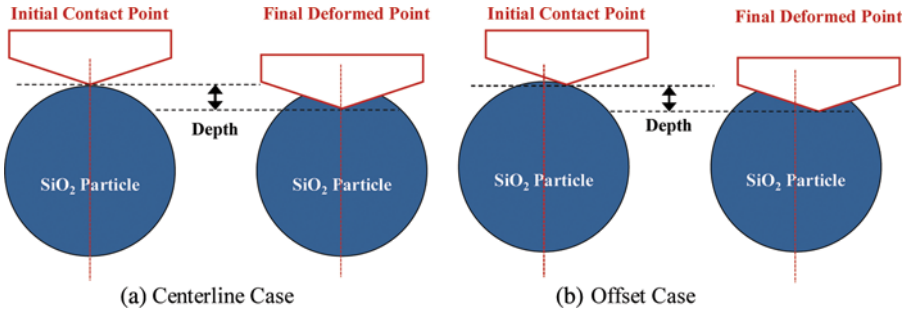

Fig. 8. Definition of penetration depth in the finite element modeling and analysis.

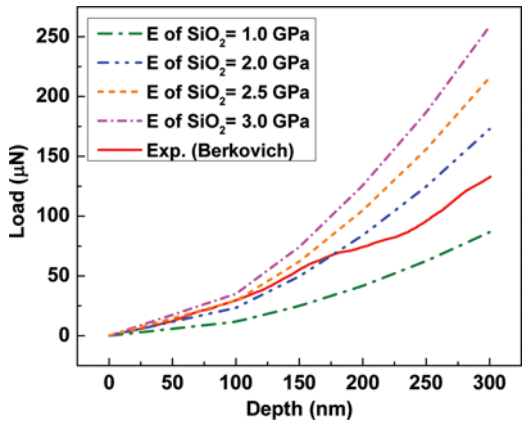

Fig. 9. Comparison of experimental load–depth curve for Berkovich indenter and SiO_2 particle with finite element predictions for various assumed values of SiO_2 particle modulus. Experiments were conducted under penetration depth control.

range 1–2.5 GPa. These values are significantly lower than the published value of the Young's modulus of bulk SiO_2 glass, which is around 73 GPa (Comte and von Stebut 2002), and the effective modulus of large numbers of SiO_2 particles embedded in a polymer matrix, which appears to be around 10 GPa (Jang et al. 2013). Given the porous nature of the particles in the current research, these results should not be surprising. For example, Herrmann et al. (2008) reported that the Young's modulus for porous thin film SiO_2 measured by nanoindentation ranged from 2.67 to 0.83 GPa, with the Young's modulus decreasing as the porosity increased. These numbers are quite consistent with the present results for nanoindentation of porous SiO_2 particles of unknown porosity. In addition, the effective particle modulus value of 10 GPa in Jang et al. (2013) does not account for the influence of viscoelastic behavior of the surrounding polymer matrix (Beake et al. 2007) and/or the effects of the particle-matrix interphase (Downing et al. 2000). The authors believe that this is the first article to report on the use of nanoindentation and finite element simulations in a combined experimental/numerical approach to determine the elastic modulus of individual porous silica particles. It is particularly encouraging that the conclusions from the two independent experiments conducted in two different laboratories and the associated finite element simulations are in such good agreement. Even with the uncertainty due to unknown tip offset in the Berkovich indenter tests as shown in Figure 7, the effective modulus values determined from Figures 9 and 10 are still in good agreement. Finally, it is clear that the flat-ended conical tip is superior to the Berkovich tip for the types of particle tests that are described here.

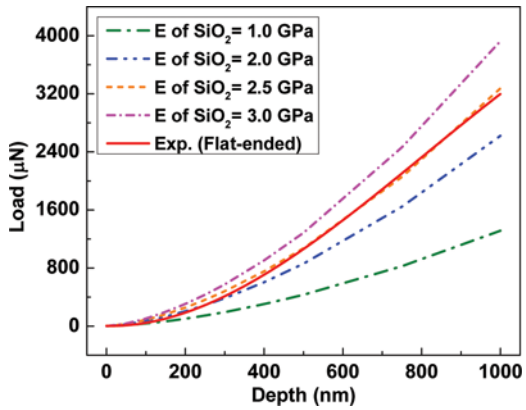

Fig. 10. Comparison of experimental load–depth curve for flat-ended conical indenter and SiO_2 particle with finite element predictions for various assumed values of SiO_2 particle modulus. Experiments were conducted under penetration depth control.

Acknowledgments

The authors would also like to thank ABC Nanotech (South Korea) for kindly providing them with the SiO_2 particles for this work, and they are also indebted to the University of Delaware Center for Composite Materials for its support.

Funding

Financial support from the National Science Foundation's Major Research Instrumentation Program Award No. 1126582 to the University of Nevada, Reno is gratefully acknowledged. The NSF Program Officer is Dr. Bruce M. Kramer. This research was partially supported by the Fundamental Technology R&D Program for Society of the National Research Foundation (NRF) funded by the Ministry of Science, ICT & Future Planning (Grant number 2013M3C8A3075845) in South Korea.

References

Beake, B. D., G. A. Bell, W. Brostow, and W. Chonkaew. 2007. Nanoindentation creep and glass transition temperatures in polymers. *Polymer International* 56(6):773–778.

Bhakri, V., J. Wang, N. Ur-rehman, C. Ciurea, F. Guiliani, and L. J. Vandeperre. 2012. Instrumented nanoindentation investigation into the mechanical behavior of ceramics at moderately elevated temperatures. *Journal of Materials Research* 27(1):64–74.

Bucaille, J. L., and E. Felder. 2002. Finite-element analysis of deformation during indentation and scratch tests on elastic–perfectly plastic materials. *Philosophical Magazine A* 82(10):2003–2012.

Caponi, S., A. Fontana, M. Montagna, O. Pilla, F. Rossi, F. Terki, and T. Woignier. 2003. Acoustic attenuation in silica porous systems. *Journal of Non-Crystalline Solids* 322:29–34.

Chang, S.-Y., and Y.-C. Huang. 2006. Nanomechanical analyses of porous SiO_2 low-dielectric-constant films for evaluation of interconnect structure reliability. *Microelectronic Engineering* 83:1940–1949.

Coquard, R., D. Baillis, V. Grigorova, F. Enguenard, D. Quenard, and P. Levitz. 2013. Modelling of the conductive heat transfer through nano-structured porous silica materials. *Journal of Non-Crystalline Solids* 363(1):103–115.

Comte, C., and J. von Stebut. 2002. Microprobe-type measurement of Young's modulus and Poisson coefficient by means of depth sensing indentation and acoustic microscopy. *Surface and Coatings Technology* 154(1):42–48.

Downing, T. D., R. Kumar, W. M. Cross, L. Kjerengtroen, and J. J. Kellar. 2000. Determining the interphase thickness and properties in polymer matrix composites using phase imaging atomic force

microscopy and nanoindentation. *Journal of Adhesion Science and Technology* 14(14):1801–1812.

Herrmann, M., F. Richter, and S. E. Schulz. 2008. Study of nano-mechanical properties for thin porous films through instrumented indentation: SiO_2 low dielectric constant films as an example. *Microelectronic Engineering* 85:2172–2174.

Herrmann, M., N. Schwarzer, F. Richter, S. Fruhauf, and S. E. Schulz. 2006. Determination of Young's modulus and yield stress of porous low-k materials by nanoindentation. *Surface and Coatings Technology* 201:4305–4310.

Huang, X., and A. A. Pelegri. 2003. Study of nano-mechanical properties for thin porous films through instrumented indentation: SiO_2 low dielectric constant films as an example. *Journal of Engineering Materials & Technology* 125(4):361–367.

Hysitron web site. 2014. http://www.hysitron.com/ (accessed February 12, 2015).

Jain, A., S. Rogojevc, S. Ponoth, N. Agrawal, L. Matthew, W. N. Gill, P. Persans, A. Tomozawa, J. L. Plawsky, and E. Simonyi. 2001. Porous silica materials as low-k dielectrics for electronic and optical interconnects. *Thin Solid Films* 398–399: 513–522.

Jang, J.-S., H. Kim, R. F. Gibson, and J. Suhr. 2013. Effective in situ material properties of micron-sized SiO_2 particles in SiO_2 particulate polymer composites. *Materials & Design* 51:219–224.

Karasinski, P., J. Jaglarz, M. Reben, E. Skoczek, and J. Mazur. 2011. Porous silica xerogel films as antireflective coatings—Fabrication and characterization. *Optical Materials* 33(12):1989–1994.

Manjunatha, C. M., A. C. Taylor, A. J. Kinloch, and S. Sprenger. 2009. The effect of rubber micro-particles and silica nano-particles on the tensile fatigue behaviour of a glass-fibre epoxy composite. *Journal of Materials Science* 44:342–345.

Oliver, W. C., and G. M. Pharr. 1992. An improved technique for determining hardness and elastic modulus using load and displacement sensing indentation experiments. *Journal of Materials Research* 7(6):1564–1583.

Page, T. F., W. C. Oliver, and C. J. McHargue. 1992. The deformation behavior of ceramic crystals subjected to very low load nanoindentations. *Journal of Materials Research* 7(2):450–473.

Simha, N. K., H. Jin, M. L. Hall, S. Chiravarambath, and J. L. Lewis. 2007. Effect of indenter size on elastic modulus of cartilage measured by indentation. *Journal of Biomechanical Engineering* 129(5):767–775.

Taylor, L. J., D. G. Papadopoulos, P. J. Dunn, A. C. Bentham, J. C. Mitchell, and M. J. Snowden. 2004. Mechanical characterization of powders using nanoindentation. *Powder Technology* 143–144: 179–185.

Uddin, M. F., and C. T. Sun. 2008. Strength of unidirectional glass/epoxy composite with silica nanoparticle-enhanced matrix. *Composites Science and Technology* 68(7–8):1637–1643.

University of Nebraska web site. 2014. http://bm3.unl.edu/hysitron-nanoindenter#details (accessed February 12, 2015).

Vandeperre, L. J., N. Ur-rehman, and P. Brown. 2010. Strain rate dependence of hardness of AlN doped SiC. *Advances in Applied Ceramics* 109(8):493–497.

Vincent, A., S. Babu, and S. Seal. 2007. Surface elastic properties of porous nanosilica coatings by scanning force microscopy. *Applied Physics Letters* 91: Article 161901.

Wypych, G. 2010. *Handbook of Fillers*. 3rd ed. Toronto: ChemTec.

Yan, W., C. L. Pun, Z. Wu, and G. P. Simon. 2011. Some issues on nanoindentation method to measure the elastic modulus of particles in composites. *Composites Part B: Engineering* 42:2093–2097.